Journal of Applied Polymer Science

REVIEW

Microstructural foundations of the strength and resilience of LLDPE artificial turf yarn

K. Ragaert, L. Delva, N. Van Damme, M. Kuzmanovic, S. Hubo, L. Cardon

Department of Materials Science & Engineering, Centre for Polymer & Material Technologies, Faculty of Engineering and Architecture, Ghent University, Technologie Park 915, Gent, 9052, Belgium

Correspondence to: K. Ragaert (E-mail: kim.ragaert@ugent.be)

ABSTRACT: The production of linear low-density polyethylene (LLDPE) yarns for artificial turf is an advanced extrusion process, which relies heavily on the polymer's semicrystalline structure and inherent strengthening mechanisms to obtain the tailored mechanical properties so typical for turf yarns: a combination of strength and resilience. This review aims to bring together all relevant aspects in the structure–materials–processing interaction triangle which is so strongly in evidence in this application, by first summarizing the specific structural origins of the properties of the semicrystalline LLDPE and then discussing how structure evolves during the different steps of the production process, to eventually come to the final product properties of the yarn. © 2016 Wiley Periodicals, Inc. J. Appl. Polym. Sci. **2016**, *133*, 44080.

KEYWORDS: extrusion; mechanical properties; polyolefins; structure–property relations

Received 5 April 2016; accepted 7 June 2016

DOI: 10.1002/app.44080

INTRODUCTION

Artificial turf is widely used, not only in landscaping (gardens, parks, and playgrounds) but also in a variety of sports applications. These include, among others, hockey,[1] rugby,[2] and soccer.[3] Artificial turf has evolved over the last decades into a highly engineered material with increasing performance and applications.[4]

The current generation of ubiquitously used artificial turf for sports applications, is the so-called third-generation pitch.[5–9] It consists of a backing onto which polymer yarns are tufted. Typically, two infill layers are added: a granulated rubber layer (e.g., styrene–butadiene rubber) and a sand layer. The upper layer, in which the yarns are unrestricted by the infill, is called the free pile layer. The polymer turf yarns are produced in polyethylene (PE), whereas previous generations were mostly polypropylene (PP) and the individual yarns are longer (typically over 50 mm) as well as spaced further apart,[8,10] which contributes to a softer feel of the turf. The material of choice for the production of the yarns nowadays is linear low-density polyethylene (LLDPE) and the production process can be either monofilament or fibrillated tape extrusion.[8,11–13]

LLDPE has a semicrystalline structure, in which the amount of crystallinity as well as the size and orientation of individual crystallites can be tailored, allowing for a large spectrum of mechanical properties.[14] Typically, yarns for artificial turf must be strong as well as resilient, meaning that they will return to an upright position after being flattened by the passing of a ball or individual. This resilience is most relevant in the free pile layer.[11,15]

Several manuscripts on the performance of artificial turf can be found in literature. However, all of these focus on other aspects, such as the biomechanical implications of turf properties[6,7,16,17] which are mostly related to the rubber infill layer[18] (i.e., loading of joints or potential athlete injuries[19,20]), functional play-related properties like coefficient of friction and play performance,[10,21,22] long-term durability[5,23] of artificial turf fields and even sustainability issues.[24–26] Also the influence of surface temperature on the mechanical properties of artificial turf is investigated.[27] Since playgrounds are also coming up as an application for artificial turf, the environmental and health issues of this green surface have been addressed in literature as well.[24,28–30]

To date, no comprehensive review has been made of the microstructural origins of the atypical set of properties within the LLDPE turf yarn itself: a combination of both strength and resilience, properties that are typically exclusive to one another.[31] Some interesting work was done on quantifying the influence of the yarn production process on the mechanical properties of LLDPE turf yarns by Kolgjini *et al.*,[8,12,13,32] but while these manuscripts offer a good description of experimental results and a first insight into the relevant aspects of polymer structure, they do not translate all the way back to basic polymer science to understand the mechanisms at work.

Kim Ragaert obtained her PhD in Polymer Engineering in 2011. She lectures materials science and polymer processing at Ghent University's Faculty of Engineering and Architecture, where she holds a tenure track position in the domain of Sustainable Use and Recycling of Polymers and Composites. Prof. Ragaert is a leading member of the Centre for Material and Polymer Technology (CPMT) at the Department of Materials Science & Engineering.

Laurens Delva is a Postdoctoral Researcher at the Centre for Polymer & Material Technologies at Ghent University, Belgium. In 2015, he obtained his PhD in Engineering from Ghent University, on the topic of (re)processing nanoclay filled polypropylene. His current research focuses on the recycling of mixed polymer waste streams and the drawing of microfibrillar composites. He also lectures to engineering students on polymer materials and material characterization.

Nicolas Van Damme is a Doctoral Researcher at the Centre for Polymer & Material Technologies at Ghent University, Belgium. In September 2014, he obtained his Master of Science in Electromechanical Engineering Technology from Ghent University. His current PhD research focuses on the processing and optimizing of recycled PET-PE blends from multilayer food trays.

Maja Kuzmanovic is a Doctoral Researcher at the Centre for Polymer & Material Technologies, at Ghent University, Belgium. She obtained her first Master in Materials Engineering with focus on biomaterials, at Faculty of Technology and Metallurgy, University of Belgrade, Serbia in July 2013. The second Master in Materials Science and Engineering, focused on nanotechnology, she obtained in July 2014 at University Carlos III of Madrid, Spain. Her current PhD research focuses on the drawing of microfibrillar composites from recycled polymers.

Sara Hubo is a senior researcher at the Centre for Polymer & Material Technologies at Ghent University. She graduated at Ghent University in 2002 as a Master in Biochemistry and has been involved in various research projects on polymer processing, more specifically defining the structure–property relationships of extruded and injection moulded (recycled) polymers.

Ludwig Cardon is the head of the Centre for Polymer & Material Technologies at Ghent University. His field of expertise is Characterization and 3D Processing of Polymers, including technologies such as injection moulding, (co-)extrusion, and 3D Printing. Prof. Cardon has more than 80 international publications at peer reviewed journals and conferences. He is the scientific chair of the biannual International Polymer & Mould Innovations (PMI) conference.

Therefore, this work aims to provide a conclusive insight into the mechanical properties of the tape yarn, how these are founded within the microstructure of the LLDPE and how they are affected—and hence can be altered—during the processing of the yarns. In a first section, some basic concepts will be revised pertaining to mechanical properties and structure of semicrystalline polymers and more specifically LLDPE. Second, the structure–property relationships for LLDPE will be elaborated and finally, the structural changes—and their effects—of the LLPDE polymer will be examined for every step within the production process of artificial turf yarns.

STRENGTH, RESILIENCE, AND STRUCTURE OF LLDPE TURF YARN

Mechanical Properties

The mechanical properties of interest for this review are mostly strength and resilience. However, aspects such as elasticity and ductility should not be neglected. The most ubiquitous test for the mechanical properties of materials is the tensile test, which leads to the engineering stress–strain diagram.[33] From the stress–strain diagram, properties such as tensile strength σ_t (maximum stress in the diagram), proportional limit σ_p (the stress up to which the elastic strain is proportional to the stress = the end of the linear area), yield strength σ_y (transition from elastic to plastic deformation), Young's modulus E (measure of the resistance to elastic deformation), and strain at break ε_b (measure of ductility) are determined.

All properties derived from the stress–strain diagram are material properties. By recalculating load and deformation to stress and strain, the dimensions of the test specimen are eliminated. This means that the massivity of a given product will not affect these properties. Yarns, however, are often quite thin products and it is difficult to test them so that material properties can be obtained. Instead, it is common in the domain of textiles to define "material properties" which are in fact dependent on the dimensions of the test specimen (often by not converting load to stress). Therefore, these are not strictly speaking material properties, but product properties. Typical examples include a yarn's dtex value and its tenacity. Likewise, resilience of turf yarns, as it is understood within the world of textiles and artificial turf, is in fact a product property instead of a material property.

In materials science, resilience is defined as the capacity of a material to absorb energy when it is deformed elastically and then, upon unloading to have this energy recovered.[33] The modulus of resilience U_r corresponds to the area under the stress–strain curve during elastic deformation, prior to yielding of the material. It may be derived that materials with (relatively) large yield strengths and low moduli of elasticity will have greater resilience. Resilience corresponds to a material's ability to absorb deflection without damage.[34,35] It is, however, not to be confused with toughness or stiffness. Stiffness is the material's resistance to elastic deformation (expressed by the Young's modulus) and toughness is the amount of energy necessary to break a section of the material. In the stress–strain diagram this corresponds to the full area under the stress–strain curve, up to the point of break. So, while resilience is a part of toughness, it is not the same. In the study of elastomers,[36,37] resilience is defined as the ratio of energy effectively regained on stress release to the original energy input. It describes the measure of return to the unbent state after forced bending of the material. For natural rubbers, this resilience value can rise up to 90%. The energy loss prohibiting the material from reaching 100% resilience is attributed to polymer chain slip.[36] When evaluating artificial turf, the second (elastomer-based) definition of resilience is used: resilience describes the ability of the monofilaments to recover from bending deformations and completely return to their initial position. While theoretically, this relates to the percentage of energy recovered, Kolgjini proposed a method[8] for measuring an equivalent, either in terms of force required to bend a monofilament to a certain position for the 10th time (dynamic measurement), or the physical recovery of the filament to the unbent position, after a certain relaxation time (static measurement).

In the dynamic method, a monofilament is subjected to 300 repetitive cycles of bending. The resilience R is expressed as the ratio between the maximal force of the last cycle of bending (F_{300}) and the maximum force (in the advancing part of the hysteresis) of the first cycle of bending (F_1)[8]:

$$R\ [\%] = \frac{F_{300}}{F_1} \times 100 \tag{1}$$

Typically, an immediate drop is observed after the first deformation, after which the relative bending force flattens out to roughly 30% of the first loading.[8]

In the static method, the deformation recovery is measured after a single deformation. A monofilament is clamped in an upright position t_0 and forcibly bent flat under a 90° angle by a plate with a force of 150 g, for 40 min. Once the plate is released, the monofilament will return to a position $\varnothing_{tx}$ after a predefined relaxation time tx (5 min, 1 h, 24 and 48 h). The deformation recovery is defined as[8]:

$$\text{deformation recovery}\ [\%] = \frac{\varnothing_{tx}}{90} \times 100 \tag{2}$$

with 90° corresponds with the perpendicular position of the monofilaments at the beginning (t_0), $\varnothing_{tx}$ the measured value of the angle at different relaxation times (tx). Note how test results will be different for different testing temperatures; deformation recovery has been found to decrease with rising temperatures.[8]

Semi-Crystalline Structure of Thermoplastics

In the conventional two-phase model illustrated in Figure 1, semicrystalline polymers consist of crystalline regions (crystallites), each having a precise alignment, which are interspersed with amorphous regions composed of randomly oriented molecules. Many bulk polymers that are crystallized from the melt form a spherulitic structure. The spherulite consists of an aggregate of ribbon like chain-folded lamellae (thickness 10 nm) radiating outward from a single nucleation site in the center of the spherulite. Each spherulite is composed of many different lamellar crystals and, in addition, some amorphous material. PE (all types) forms a spherulitic structure when crystallized from the melt. The unit cell of the crystallites is orthorhombic ($a \neq b \neq c$ and $\alpha = \beta = \gamma = 90°$). This orthorhombic structure

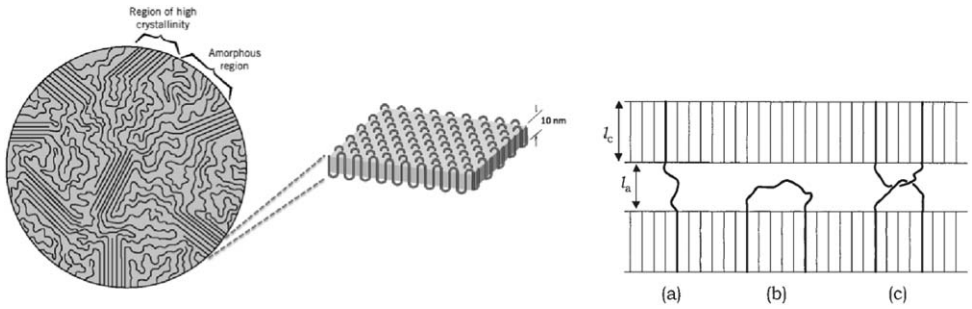

Figure 1. (Left) Schematic representation of the structure of a semicrystalline polymer in the two-phase model (adapted from ref. 38) . (Right) Schematic representation of (a) a TM, (b) a loose loop, and (c) an entangled loop.[39]

can be identified and quantified by a specific band in Raman spectrometry.[39–41] Some relevant definitions include:

- Crystallinity (percentage) α_c: the fraction of crystalline phase in the polymer;
- Lamellar thickness l_c: the (average) thickness of the crystalline lamellae;
- Amorphous thickness l_a: the (average) thickness of the amorphous regions between the crystalline lamellae.

The different layers are held together with tie molecules (TMs) through the amorphous phase. TMs are chains that belong to two adjacent crystallites crossing the amorphous phase.[42–44] So the chain must have a minimal length (L) of $2^*l_c + l_a$. TMs are also called "bridges" in some literature.[45–47] In this manuscript, both terms will be used indiscriminately. Other known structures are loose loops (which loop back into the original crystallite) and entangled loops (which also loop back, but are entangled with a loop from another crystallite). They are important to connect the different crystallites. Finally, there are the so-called tails, which are part of the crystallite, but have chains ending in the amorphous region.[48,49]

Structure of LLDPE

LLDPE is a variant of PE, consisting of a linear main chain with several short-chain branches. So the conformation of the chain-structure is situated between the linear structure of high-density polyethylene (HDPE) and the long-chain branched structure of LDPE, as is illustrated in Figure 2. This configuration will affect the density and crystallization behavior of the polymer. The amount and homogeneity of branching is a critical factor in the process of crystallization and has to be studied for a good understanding of the crystallinity. For an overview of polymer reaction engineering of PE and modeling of polymerization reactions, we refer to literature.[50,51]

Influence of Polymerization on Structure. The use of metallocene catalysts in the polymerization process offers great advantages over the conventional Ziegler–Natta catalysts. Especially, the homogeneity of branching makes it very interesting. The LLDPE can be tailored in a regular way, so the polydispersity of the branching becomes very narrow and the crystallization process can be much more controlled.[50,52,53] The regularity of the metallocene process will realize an uniform distribution of the different monomers, while the use of the Ziegler–Natta catalyst creates a complex incorporation of the different monomers with a broad polydispersity as result.[54,55]

It is well known that branching is a key factor in determining the performance and processability of a polymer product. There are two types of branching in polyolefines, short-chain branching (SCB) and long-chain branching. SCB is formed by incorporating α-olefins (e.g., 1-butene, 1-hexene, and 1-octene) into the PE or PP main chains. In industry, this is often referred to as C3, C4, C6, or C8 LLDPE, wherein *cx* denominates propene, butene, hexane, or octane, respectively. These result in the following side groups, respectively: methyl, ethyl, butyl, and hexyl. SCB causes steric hindrance on the polymer chains, which obstructs the formation of the crystalline lamellae, as only the methyl groups are small enough to be a part of the inner core of the crystals. Hence, SCB actively reduces crystallinity in the polyolefin.

Branching within the LLDPE will depend on the chain length of the molecule that was used as a PE-(α-polyolefin) copolymer precursor for polymerization.[56] However, in general, the most important factor for the crystallization percentage α_c is the amount of branches, expressed in mole % branch points.[57] The number of branch points will likewise have substantial influence on the crystallite thickness: l_c decreases with increasing mole % branch points, as chains become more difficult to fold into the crystalline lamellae. Common values are 12 nm for a linear PE to 4 nm for a highly branched (4–5 mol % branching points) PE.[57] Finally, the branch density will affect the formation of TM and entangled loops within the semicrystalline structure.[58,59] As

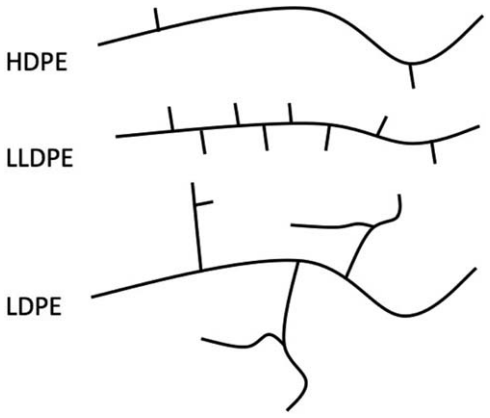

Figure 2. The chain structures of HDPE, LLDPE, and LDPE.

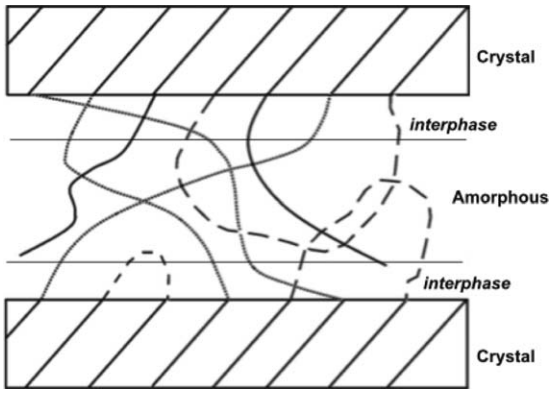

Figure 3. Principle of the interphase, with bridges or TM (gray solid), loops (dashed), and tails (solid).[61]

the branches of LLDPE do not take part in the crystallite formation; a decrease of l_c follows from a larger branch density. This in turn makes it easier to form TM.

Occurrence of Third Phase. The basic two-component model of crystalline lamellae, interspaced with an amorphous region, is not sufficiently nuanced to account for the microstructural properties of LLDPE yarns. The main inadequacy of this model is that it would require a severe discontinuity in molecular order at the crystalline-amorphous boundary, where polymer chains would abruptly go from a highly ordered to an unordered state.[60] Instead, it is widely accepted that a third phase, of intermediate order, exists at the interface between crystalline and amorphous regions.[44,60–63] Within this third phase, the chains emerge from the lamellae with a high degree of molecular alignment, which gradually decreases in terms of density and orientation.[45,64] This phase is referred to by any of the following terms: semiordered, intermediate, rigid amorphous, interfacial, interzonal, interphase, and transitional zone.[60] Within this work, we shall refer to it as interphase or third phase. The principal appearance of the interphase is shown in Figure 3.

It has been proven that the polymer chain stems emerging from the lamellae are not orthogonal in orientation to the basal plane of the lamellae. This so-called chain tilt will affect the density and topology of the interphase.[44] The third phase does not occur in all semicrystalline polymers, but it is far more likely to exist in highly oriented polymers (like cold drawn yarns) than unoriented samples.[60] As such, it will prove elementary in the understanding of the crystalline growth within cold-drawn LLDPE yarns, even if the exact morphology of the third phase remains a topic for discussion.[45]

STRUCTURE–PROPERTY RELATIONSHIPS IN LLDPE

Deformation Mechanisms

As previously discussed, semicrystalline polymers are composed of an amorphous phase interlayered with crystalline lamellae. The macromolecular chains are however engaged in both phases, which complicates the deformation mechanisms.[65] There are three, currently recognized, principal modes of deformation of the amorphous phase in semicrystalline polymers: interlamellar slip, interlamellar separation, and stack rotation.[66,67] Interlamellar slip involves shear of the lamellae parallel to each other with the amorphous phase undergoing shear. This mode of deformation is illustrated in Figure 4(a). It is a relatively easy mechanism of deformation for the material above the glass transition temperature T_g: the elastic part of the deformation can be almost entirely accounted for by reversible interlamellar slip. Interlamellar separation, illustrated schematically in Figure 4(b), is induced by a component of tension or compression parallel to the lamellae themselves. Stack rotation is illustrated schematically in Figure 4(c). Any other deformation of the amorphous phase requires a (plastic) change in the crystalline lamellae.[68] Crystallites undergo plastic deformation of crystallographic type under the action of external force through dislocation mechanisms.[65,69]

The plastic deformation of polymer crystals is generally expected to be crystallographic in nature and to take place without destroying the crystalline order. The only exception to this appears to be at very large deformation, when cavitation and voiding take place and crystals may be completely broken down and new crystals may form with no specific crystallographic relationship with the original structure.[66,70] Polymer crystals can deform plastically by crystallographic slip,[71] by twinning and by martensitic transformation.[66,72,73] The slip mechanism is the most important.

Crystallographic slip is the main deformation mode up to moderate strains, and occurs by gliding of macromolecular chains along each other on crystallographic slip planes within the crystalline lamella. When the direction of slip is parallel to the chain

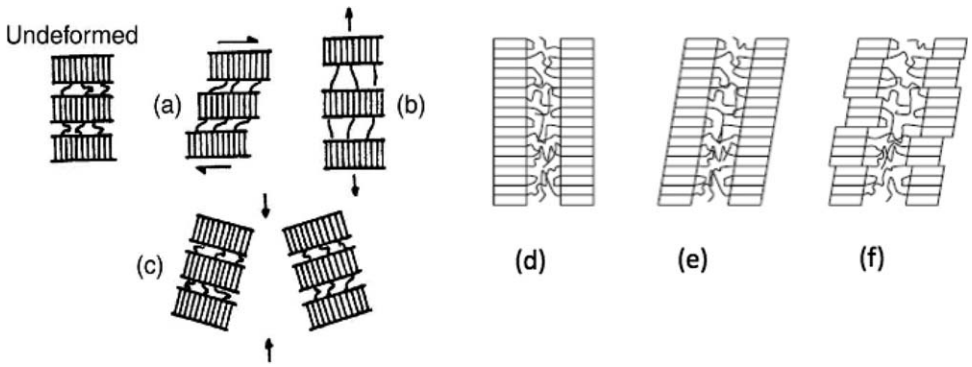

Figure 4. (Left) Different deformation mechanisms in the amorphous phase.[66] (a) Interlamellar slip, (b) interlamellar separation, and (c) stack rotation. (Right) Fine and coarse slip in the crystalline phase[74]: (d) undeformed lamella; (e) fine slip; and (f) coarse slip.

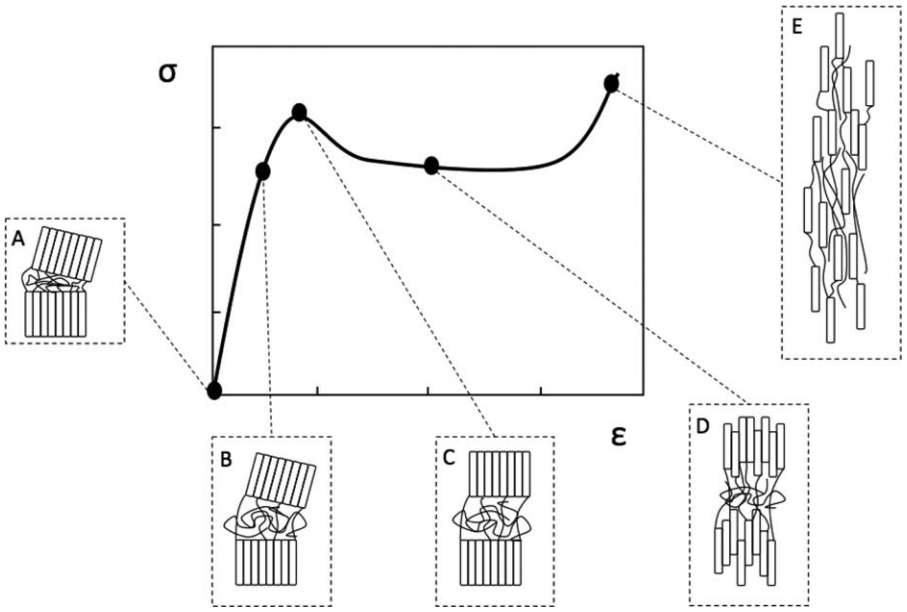

Figure 5. Typical stress–strain curve of semicrystalline polymers and the resulting structural changes.

axis, the deformation mechanism is referred to as chain slip, whereas when the slip direction is perpendicular to the chain direction, the slip mechanism is called transverse slip.[63,71] During the early stages of deformation, plastic deformation predominantly occurs by fine slip, where a small amount of deformation is equally distributed on a large number of slip planes. At larger strains, fine slip is accompanied by a process of coarse slip, with large deformations on a few slip planes, resulting in the break-up of crystalline lamellae.[74] These two slip mechanisms are schematically illustrated in Figure 4(e,f), with Figure 4(d) representing the undeformed structure. Coarse slips are responsible for the formation of block structures from continuous lamellae and their fragmentation, fine slips change the orientation of lamellar planes in relation to the direction of macromolecular chains in crystals.[65]

Structure Development during Deformation

The structure of semicrystalline polymers (combination of interconnected amorphous and crystalline segments) undergoes different changes during deformation.[75–77] These are illustrated in Figure 5. The important points on the stress–strain curve are highlighted and the structural changes related to each of them are shown in the figure.

1. Undeformed structure: No deformation yet, structure is intact. Both amorphous and crystalline regions are undeformed.
2. Up to σ_p—amorphous regions elongate: During the first stage of the deformation, up to the proportional limit, the amorphous regions elongate induced by the different amorphous slip phenomena. This deformation is reversible and facilitates the elastic deformation.
3. σ_p to σ_y—crystalline regions align: the constraints imposed by the lamellae imply that only limited deformation can be accommodated by the amorphous phase. With an increase of load, the stress–strain dependence becomes nonlinear and inelastic deformation occurs: the crystalline regions align themselves to the direction of the applied stress. This is irreversible, plastic deformation and the mechanism used is that of fine slip.[78]
4. Beyond σ_y—crystalline block segments are sheared apart: Once σ_y is reached, coarse slip will occur within the crystalline lamellae.[47,78] The lamellae are effectively sheared apart into smaller crystalline block segments. This deformation is plastic. Engineering stress decreases, due to neck formation. True stress will continue to rise.
5. Final separation of crystalline block segments: The crystalline segments continue to fragment and finally separate into a fibril-like structure: bridge and entanglement chains as well as third phase regions in the amorphous phase resist this, which leads to a strain-hardening effect.

Relationship Structure–Mechanical Properties

Mechanical Strength in the Two-Component Model. The yield stress is related to the onset of plastic deformation, of which we have already discussed that it is carried by the (fine and coarse) slip in the crystalline regions. This infers that anything, which increases the crystalline region's resistance to this slip, will heighten the value of σ_y. Foremost among these are crystallinity α_c and lamellar thickness l_c. Larger, bulkier crystalline regions will display higher resistance to yielding. The relation between l_c and σ_y has been observed, by Brooks and Mukhtar for HDPE and for l_c up to 28 nm.[79] These were later validated by and expanded upon for l_c values up to more than 150 nm by Kazmierczak *et al.*[80] They concluded that the increase of yield stress with crystalline thickness is only valid up to values of 40 nm. Beyond this value, an obvious plateau is observed in the curves. There is no explanation as of yet for this apparent limit.[80]

The structural relations of elastic modulus E are somewhat more complex to define in a straightforward manner: it is not dependent on a single characteristic.[66] As E is the slope of the linear region, the end point of this region is determined by σ_p,

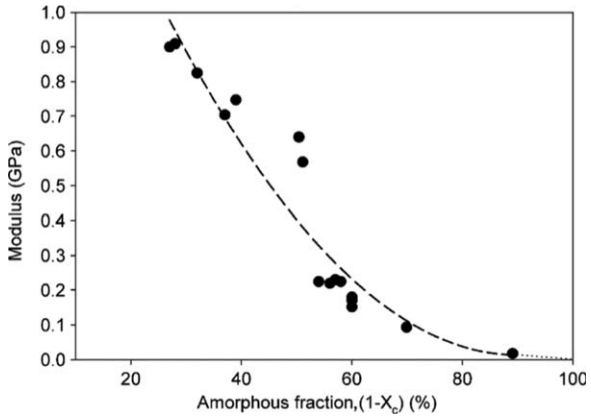

Figure 6. Young's modulus as a function of amorphous fraction size for different PE polymers.[82] α_c is noted as X_c.

which is near or equal to σ_y. Therefore, anything that will increase σ_y, will logically affect E, as the slope will become steeper. However, as the deformation in the elastic region is governed by the elongation and alignment of the amorphous section, the amorphous fraction will also influence E. Typically, a smaller amount of amorphous polymer chains implies a reduced ability for elastic straining, thereby decreasing strain at yield ε_y and increasing E. So an increase in α_c will have a combined effect on E, by simultaneously increasing σ_y via the larger crystalline fraction and reducing ε_y via the smaller amorphous fraction. The relationship between E and α_c has been quantified for high-crystalline values in HDPE by Galeski[66]: large increases in E can be achieved, especially in the region between 70 and 80% crystallinity. This was also confirmed by Martin *et al.*[81] An upward trend was obvious, but no truly linear relation could be established. However, these are quite high values for α_c, which are typically not reached with LLDPE. A broader range of PE polymers, including some LLDPE types, were investigated by Bartczak and Kozanecki.[82] Their results are shown in Figure 6. They confirmed the clear, albeit nonlinear, relationship between the growing size of the amorphous fraction and the decreasing modulus.

Generally, it may be concluded that E modulus will increase significantly with increasing crystalline fraction.

Influence of Third Phase. The third phase is partially ordered and anisotropic with properties intermediate to those of the crystalline and amorphous phase.[83] The chains in the third phase are stretched, but lack lateral order. It is necessary at this point to introduce the concepts of trans and gauche conformation within PE. Conformation describes spatial geometry of side groups (in this case the methyl group) that can be changed by rotation and flexural motion. It is defined by the projected alignment of the side groups.[84] When they are in the trans conformation, they are fully opposed (angle 180°); this is the most favorable energy state. When they are in the gauche conformation (angle + or − 60°), their energy state is less favorable. Typically, regions of higher order are in the trans conformation and region of less order are in the gauche conformation. In the third phase, both trans and gauche conformations occur. Their occurrence can be verified by IR spectrometry[85] or NMR experiments.[64]

Kolgjini *et al.* found a relation between the amount of trans conformation in the third phase and the E modulus of the whole LLDPE yarn[32]: as trans conformation increases, the now more-ordered third phase becomes more resembling to a crystalline region and E modulus increases. This resemblance is also reported by Martin *et al.*[81]

In similar research, it was found that there is a specific IR band (1130:1160 cm^{-1}) which reflects the degree of orientation within PE chains and that the increase of this band was nearly linearly related to an increase of E modulus.[86]

Resilience. Resilience was previously defined as the ability of the yarn to recover from (theoretically elastic) bending deformations. This recovery is governed by the return of the amorphous fraction to an undeformed (unelongated) state. Therefore, a larger amorphous phase will increase the resilience and deformation recovery of the yarn.[8] Hence, all effects that will increase the mechanical strength by increasing the crystalline fraction, automatically reduce the amorphous fraction and thus limit the possibilities for resilient behavior. An extra degree of crystallinity will adversely affect resilience and deformation recovery.[13] This essentially makes the property mutually exclusive with mechanical strength, much as with the classical conflict between hardness and ductility.

STRUCTURE DEVELOPMENT DURING PROCESSING OF ARTIFICAL TURF YARN

For semicrystalline polymers, a large amount of attention has been given to the microstructural changes during mechanical treatments because it could gain more insight into the molecular mechanisms of plastic deformation and provide possible routes for improvement of the material. From an engineering point of view, it is essential to understand the physical orientation process and to control the orientation state of both the crystalline and the amorphous phases during industrial operations such as fiber spinning, film blowing, injection molding, and melt drawing. Knowledge about the heterogeneous deformation process of spherulitic structure and changes of microstructure is really indispensable. The products in real-life applications are often utilized under varying temperatures, and many procedures used in industry are conducted at elevated temperatures to reduce testing time.[87] Key scientific issues for production of oriented polymers with enhanced properties include the chemical structure of the polymer and its degrees of regularity and the plastic deformation.[88]

Production of LLDPE Artificial Turf Yarn

A schematic representation of the processing steps in the fabrication of artificial turf yarns is given in Figure 7. Some typical temperatures and parameters are described for a LLDPE with a melt temperature of 124 °C.[13]

After the actual extrusion of the LLDPE monofilaments through a spinneret mould, the yarn passes through the following consecutive steps:

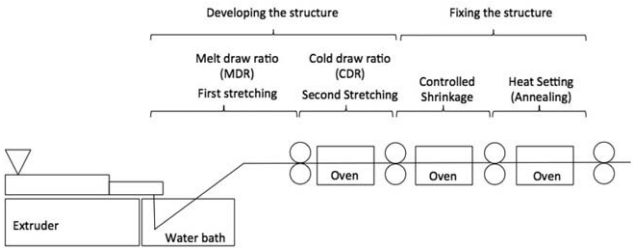

Figure 7. Typical processing steps for the production of artificial turf yarn. (adapted from Ref. 8.)

1. Melt drawing (first stretching): orientation of polymer chains even before the solidification of the extruded polymer will allow for greater crystallization during the solidification of the yarn structure;
2. Cold drawing (second stretching)—95 °C: strain hardening and development of an oriented fibrillar crystalline structure, amount of which is dependent on cold draw rate;
3. Controlled shrinkage (annealing with varied ends)—15% at 120 °C: an elevated temperature and an adapted speed of the rolls make it possible for the filaments to shrink in a controlled way;
4. Heat setting (annealing with fixed ends)—10 s at 120 °C: reduction of internal stresses.

Structural Development during Processing

Melt Drawing. As the polymer is solidifying after extrusion, it is drawn through the water bath. Mobility of polymer chains in the liquid state is high and this first stretching step allows for both a first reduction of filament size after the spinneret and an orientation of the polymer chains along the stretching direction. Here, the draw temperature will influence the speed of this process.[89] As was discussed earlier, crystallization is facilitated by higher degrees of order. This preorienting of the polymer chains will allow for greater crystallization in the structure of the solid polymer. The resulting crystallinity will also be affected by the amount of defects present in the polymer structure. As chain defects are commonly excluded from crystalline growth, the length of crystallizable methylene sequences is reduced with increasing defects.[90]

At the end of the melt drawing, the polymer is completely solid and will remain so for the further steps of the process.

Cold Drawing. If we consider the cold drawing as the ith step in the process, then the following definitions can be made:

$$\text{Stretch ratio } \lambda = \frac{l_{i+1}}{l_i} \tag{3}$$

$$\text{Cold draw ratio CDR} = \frac{f_{i+1}}{f_i} \tag{4}$$

With l_i the length of the yarn after the ith step and f_i the corresponding yarn cross section.

The stretch ratio is a measure for the elongation of the yarn, while the CDR is a measure for the necking (thinning of cross section) of the yarn. In general, cold drawing means the plastic deformation of materials at temperatures where no structural reorientation can occur. For polymers, this was originally defined for amorphous polymers, which were stretched in a temperature range between the brittle point and glass transition,[91] meaning there can be no molecular mobility. Necking is a typical phenomenon for cold drawing. Semi-crystalline polymers, however, can also deform with necking at temperatures that are considerably higher than their glass transition, if the strain rate is sufficiently high. The upper temperature limit for this is the temperature T_h, above which supermolecular mobility is possible.[92] Crystallites are such supermolecular elements: above T_h they will individually shear off one another instead of fracturing into smaller blocks (fibrillation), which is responsible for the strain hardening effect.[93] T_h approximately equals 0.8–0.9 of the melting point of a polymer on a Kelvin scale. Above T_h, but lower than the melting point, hot drawing is realized (no plastic deformation and fibrillation).

For semicrystalline polymers, cold drawing is associated with a large strain, resulting in a large amount of plastic deformation, but with some portion of elastic deformation.[94] The structure development during cold drawing of semicrystalline polymers will now occur within the yarn[88,95,96]:

i. Elongating of amorphous phase (including third phase) = elastic deformation
ii. Alignment (tilting) of crystalline regions through fine slip = plastic deformation
iii. Shearing of crystalline regions into smaller blocks by coarse slip = plastic deformation
iv. Further aligned shearing into a fibrillated structure = plastic deformation

Cold drawing will significantly increase E modulus, as well as reduce resilience and deformation recovery. These effects are more pronounced for higher CDR values.[8]

Note how the amount of crystalline phase α_c will not change significantly during cold drawing. However, its morphology does change. First, the individual crystallites become smaller as they are fractionated during fibrillation.[95,97] Also, the orthorhombic lattice of the LLDPE will partially undergo a solid state transformation to a monoclinic lattice ($a \neq b \neq c$, $\alpha = \beta = 90° \neq \gamma$).[98–100] These crystals are slightly less dense, as it is believed the lattice parameter a will increase.[101]

The orientation of the (already more ordered) third phase also increases during the cold drawing. The TMs are stretched taut and it has been found that trans conformation will increase,[32,96,100] which further contributes to higher levels of order and increased modulus.

The resulting structure is not an equilibrium state and contains elastic deformation (of the amorphous phase). If the yarn were to be subjected to elevated temperatures afterwards, it would shrink considerably as the amorphous fraction returns to its unstressed, nonaligned state. Such residual shrinkage is undesirable for further processing of the yarn by tufting or weaving. Implementing controlled shrinkage and annealing steps in the process will mitigate residual shrinkage.

Controlled Shrinkage. Shrinkage causing curling or inhomogeneous performance of yarn is undesired in the process of

artificial turf production and backing as well as in the installed field. Stretched tapes have a high degree of polymer orientation. The distributed crystal phase is connected by the stretched polymer chains of the tie chains. Thermally activated, these out-of-equilibrium polymer chains start to retract towards an equilibrium, random state. As this amorphous phase shrinks back to an unstretched state, so the polymer yarn will shrink. The potential amount of shrinkage can be related to the density of the polymer. Lower-density LLDPEs have smaller crystalline fractions, resulting in longer amorphous phases, which will retract more upon shrinkage. This was experimentally confirmed by Sandkuehler.[102] Liu *et al.* showed the same effect for industrial PET yarns.[103] Hence, residual shrinkage can be somewhat mitigated by working with high-density polymers.

Controlled shrinkage in the process has two benefits:

Reduction of residual shrinkage in further processing of the yarn into artificial turf

Prerequisite for crystalline growth during the annealing step

In a controlled shrinkage step, the roll speeds are controlled so that the yarn can only shrink a preset amount. A typical value is 15%.[13] After the controlled shrinkage step, the level of orientation in the polymer will have been reduced (mainly in the amorphous and third phase). So even if the overall crystallinity of the polymer remains the same, there will be a decrease in mechanical strength but also some return of resilience and deformation recovery.[13]

Annealing (Fixed Ends). The final step in the process is the so-called heat setting or annealing with fixed ends ($l_{i+1} = l_i$). This occurs at temperatures near (yet still below) the melt temperature of the polymer. Postcrystallization of LLDPE will occur and is highly dependent on the applied temperature.[104] The crystallization kinetics are function of the crystal growth rate (in μm/s) and the induction time (time to reach stable nucleus, in s). These two can be joined together in one dimensionless Avrami Growth Dimension. It was found by Liu *et al.* that this value maximizes near 110 °C for LLDPE.[104] Also Patel mentions a high crystallization half time for a crystallization temperature of 110 °C.[105] This means that with an oven temperature of 120 °C (estimated yarn core temperature of 110 °C), thermodynamic conditions are optimal for (re)crystallization.

In polymer processing, annealing of semicrystalline polymers is generally considered to be an effective method to modify the microstructure and promote the mobility of molecular chains toward a more thermodynamically stable state, resulting in a profound enhancement of the properties.[31] For yarns, which have previously been cold drawn and then allowed (controlled) shrinkage, this is especially effective.

During annealing, different changes in crystal morphology occur depending on temperature and polymer. The first phenomenon is the perfection of primary crystals. In other words, the activated molecular chains (due to temperature and previous shrinkage) in unstable crystals or amorphous (and third) phase tend to rearrange into the primary lamellae, leading to higher crystalline perfection.

The second phenomenon is the recrystallization process. The existing crystalline blocks will thicken and new, smaller, crystallites will come into existence as well. Thus, α_c will rise. This occurs at the expense of existing small crystals (the existing tiny and imperfect crystals have by definition a lower melting temperature T_m and thus will first melt and then recrystallize into new stable crystals) as well as portions of the amorphous phase. Additionally, the partial transformation of the orthorhombic configuration to a monoclinic structure, achieved during cold drawing, is reversed and the orthorhombic crystallinity is restored.[95]

As a result of the increased crystallinity, modulus will once more rise (but not to the level of the cold drawing step) and resilience properties will decrease slightly.

It is important to note that controlled shrinkage is absolutely mandatory before the annealing step. Without the controlled shrinkage, the amorphous phase would not have been able to relax and would create internal stresses during annealing leading to a thermodynamically unstable structure and obstructing the new crystallization. It has been experimentally confirmed that there is no significant crystalline growth during annealing with fixed ends if the shrinkage step is skipped.[13]

DIRECTION OF THE FIELD

During recent years, most research concerning the production and/or use of artificial turf has been focused on the improvement of the comfort for the consumer. The main concern is finding solutions for the abundant skin-turf friction injuries compared to natural grass. Tay *et al.*[1] for example tried determining the importance of the various components in the overall skin-friction behavior using the standardized Securisport testing device. They concluded that improvements in the reduction of friction from the fiber yarns may be more of a priority than adapting the infill. The shape of the filament itself has also been topic of recent research and could possibly reduce this friction coefficient.[106] In addition to the friction coefficient, the surface temperature of artificial turf is also very different than that of natural grass. Villacañas *et al.*[107] studied how various structural components such as the type of fiber, the type of infill, the age of the turf and the hours of use influence the surface temperature. Other researchers are developing non disclosed infrared reflective coatings.[108] Furthermore, research projects such as the Wetgrass project[109] coordinated by CITEVE have aimed at developing new turf systems with reduced surface temperatures and lower skin-turf friction. The (commercial) importance of the comfort for the turf user is not only illustrated by research on skin injuries, but also by the research on the biomechanical behavior of the turf under complex loading conditions.[110,111] This research connects the fundamental materials science of the composing materials with the user interactions.

Another concern recently addressed is the long term behavior of artificial turf. The degradation of the materials for example is part of the research of Fleming *et al.*[112,113] Other aspect is the long term variation of surface hardness across an installed artificial turf pitch. Forrester and Tsui[114], for example, investigated the role of maintenance in minimizing this issue.

Table I. Summary of the Structural and Property Changes in LLDPE Turf Yarn During Processing

Process step		Cold drawing	Contr. shrinkage	Heat set (fixed ends)
What happens in the structure?	Crystal phase	Alignment (fine slip—plastic) Fibrillating into smaller blocks (coarse slip-plastic)	/	Perfection of primary crystals Recrystallization Rise in crystallinity
	Amorphous phase	Alignment and elongation (elastic)	Deorientation	Total amount lowers
How does this affect the property?	Crystallinity (α_c)	—	—	↑
	Stiffness (*E*)	↑↑↑	↓↓	↑
	Resilience (*R*)	↓↓↓	↑↑↑	↓

Finally, more and more questions are raised about the environmental and health impact of artificial turf. An excellent review has been written on this topic by Cheng *et al.*[24] However, it has to be highlighted that end-of-life properties in terms of recyclability of newly designed turfs have to be considered. Recycling schemes are being developed and consist mostly of separation of the monofilaments from the other constituents and reprocessing them into new materials.[24,115]

The fact that most of the (published) academic research focuses not on the material science of the turf, but on its interaction with the user (mostly sportsmen), is symptomatic of the fact that the larger part of research and development of the turf materials (yarn, infill, and ground layer) is conducted by the manufacturers. They typically keep their results close to their chest, which limits the transfer of information. This provokes a certain mismatch and misunderstanding between industry and research which will need to be addressed. By presenting the current review, the authors have attempted to close this gap a little by summarizing the necessary insights into the development of structure and properties during the different processing steps in the production of artificial turf yarns.

To further address the improvement of the performance of the yarn materials themselves, an extensive and fundamental quantification of the described structural changes in each step of the artificial turf production, would be most useful. The specific influence of each material and processing parameter (temperatures, stretch ratios, and molecular structure) should be mapped in an ambitious design-of-experiments set-up. Furthermore, concerning the shape of the filaments, an extensive rheological analysis of the polymer flow through the differently shaped extrusion dies would contribute significantly to the understanding of how the die shape affects the orientation of the melt and the structures developed in further processing. Finally, the effect of these structural aspects on the surface properties, friction foremost among them, should continuously be taken into account throughout such experiments, as this is a major aspect for the user comfort.

CONCLUSIONS

A summary of the different process steps (after melt drawing, during which the high degree of orientation allows for greater α_c than unstretched polymer) in the production of LLDPE yarns for artificial turf is given in Table I. The Table summarizes the effects within the different structural phases and the resulting changes in properties. Note how the amount of crystallinity α_c does not change significantly throughout the cold drawing (while its morphology does) and shrinkage steps.

It has been discussed how *E* modulus is largely attributed to the crystalline fraction and resilience is related to the ability of the amorphous fraction to return to an unstretched state. Therefore, as a rule-of-thumb, it can be observed that all structural changes that increase α_c (which inherently reduces the amorphous fraction) will increase *E* modulus and decrease resilience properties.

The initial effects of the cold drawing step will increase with higher CDR, as the fibrillation of the crystalline structure and taut stretching of amorphous chains will be more pronounced.

ACKNOWLEDGMENTS

This study was funded by the Faculty of Engineering and Architecture of Ghent University.

REFERENCES

1. Tay, S. P.; Fleming, P.; Forrester, S.; Hu, X. *Proc. Eng.* **2015**, *112*, 320.
2. Ferrandino, M.; Forrester, S.; Fleming, P. *Proc. Eng.* **2015**, *112*, 308.
3. Rodrigues, L.; Rosendo, H.; Silva, S.; Durães, N.; Moura, B.; Silva, R.; Moreira, A. *Tech. Text.* **2016**, 59.
4. Aldahir, P.; McElroy, J. *Agron. J.* **2014**, *106*, 1297.
5. Fleming, P. R.; Forrester, S. E.; McLaren, N. J. *Proc. Inst. Mech. Eng. Part P: J. Sports Eng. Technol.* **2015**, *229*, 169.
6. Williams, S.; Hume, P. A.; Kara, S. *Sports Med.* **2011**, *41*, 903.
7. Sanchez-Sanchez, J.; Garcia-Unanue, J.; Jimenez-Reyes, P.; Gallardo, A.; Burillo, P.; Luis Felipe, J.; Gallardo, L. *PLoS One* **2014**, 9.
8. Kolgjini, B.; Schoukens, G.; Kiekens, P. *J. Appl. Polym. Sci.* **2012**, *124*, 4081.
9. Tay, S. P.; Hu, X.; Fleming, P.; Forrester, S. *Mater. Des.* **2016**, *89*, 177.
10. Taylor, S. A.; Fabricant, P. D.; Khair, M. M.; Haleem, A. M.; Drakos, M. C. *Phys. Sports Med.* **2012**, *40*, 66.

11. Sandkuehler, P.; Torres, E.; Allgeuer, T. *Engineering of Sport 8: Engineering Emotion - 8th Conference of the International Sports Engineering Association (Isea)* **2010**, *2*, 3367.
12. Kolgjini, B.; Schoukens, G.; Shehi, E.; Kiekens, P. *Fibres Text East Eur.* **2013**, *21*, 23.
13. Kolgjini, B.; Schoukens, G.; Kola, I.; Rambour, S.; Shehi, E.; Kiekens, P. *Autex Res. J.* **2014**, *14*, 187.
14. Wang, Y.; Ge, S.; Rafailovich, M.; Sokolov, J.; Zou, Y.; Ade, H.; Luning, J.; Lustiger, A.; Maron, G. *Macromolecules* **2004**, *37*, 3319.
15. Hufenus, R.; Affolter, C.; Camenzind, M.; Reifler, F. A. *Macromol. Mater. Eng.* **2013**, *298*, 653.
16. Zanetti, E. M.; Bignardi, C.; Franceschini, G.; Audenino, A. L. *J. Sport Sci.* **2013**, *31*, 767.
17. Drakos, M. C.; Taylor, S. A.; Fabricant, P. D.; Haleem, A. M. *J. Am. Acad. Orthop. Surg.* **2013**, *21*, 293.
18. Sánchez-Sánchez, J.; Felipe, J. L.; Burillo, P.; del Corral, J.; Gallardo, L. *Proc. Inst. Mech. Eng. Part P: J. Sports Eng. Technol.* **2014**, *28*, 155.
19. van den Eijnde, W. A.; Peppelman, M.; Lamers, E. A.; van de Kerkhof, P. C.; van Erp, P. E. *Orthop. J. Sports Med.* **2014**, *2*, 2325967114533482.
20. Bianco, A.; Spedicato, M.; Petrucci, M.; Messina, G.; Ewan, T.; Sahin, F. N.; Paoli, A.; Palma, A. *Asian J. Sports Med.* **2016**, 7.
21. McLaren, N. J.; Fleming, P. R.; Forrester, S. In Engineering of Sport 10; James, D.; Choppin, S.; Allen, T.; Wheat, J.; Fleming, P., Eds., Elsevier, Sheffield, UK, **2014**.
22. Nedelec, M.; McCall, A.; Carling, C.; Le Gall, F.; Berthoin, S.; Dupont, G. *J. Sport Sci.* **2013**, *31*, 529.
23. Martin, J. M.; Sandkuehler, P. Google Pat. (**2015**).
24. Cheng, H.; Hu, Y.; Reinhard, M. *Environ. Sci. Technol.* **2014**, *48*, 2114.
25. Stiles, V. H.; James, I. T.; Dixon, S. J.; Guisasola, I. N. *Sports Med.* **2009**, *39*, 65.
26. Henry, E. M.; McMains, T. J.; Sanchez, T. R. Google Pat. (**2012**).
27. Charalambous, L.; und Wilkau, H. C. V. L.; Potthast, W.; Irwin, G. *J. Sport Health Sci.* **2015**, article in press.
28. Pavilonis, B. T.; Weisel, C. P.; Buckley, B.; Lioy, P. J. *Risk Anal.* **2014**, *34*, 44.
29. Menichini, E.; Abate, V.; Attias, L.; De Luca, S.; Di Domenico, A.; Fochi, I.; Forte, G.; Iacovella, N.; Iamiceli, A. L.; Izzo, P.; Merli, F.; Bocca, B. *Sci. Total Environ.* **2011**, *409*, 4950.
30. Ginsberg, G.; Toal, B.; Kurland, T. *J. Toxicol. Env. Heal.* **2011**, *A74*, 1175.
31. Shi, S. Y.; Pan, Y. M.; Lu, B.; Zheng, G. Q.; Liu, C. T.; Dai, K.; Shen, C. Y. *Polymer* **2013**, *54*, 6843.
32. Kolgjini, B.; Schoukens, G.; Kiekens, P. *Int. J. Polym. Sci.* **2011**.
33. Callister, W.; Rethwish, D. *Fund. Mater. Sci. Eng.*; Wiley: Hoboken, USA, **2013**.
34. Ashby, M.; Johnson, K. Materials and Design; Elsevier: Oxford, UK, **2007**.
35. Hosseini, S.; Barker, K.; Ramirez-Marquez, J. E. *Rel. Eng. Syst. Saf.* **2016**, *145*, 47.
36. Houwink, R.; De Decker, H. K. Elasticity, Plasticity and Structure of Materials; Cambridge University Press: Cambridge, UK, **1971**.
37. Siviour, C. R.; Jordan, J. L. *J. Dyn. Behav. Mater.* **2016**, *2*, 15.
38. Callister, W. D. Materials Science and Engineering, 8th ed.; John Wiley & Sons, Ltd: Hoboken, USA, **2010**.
39. Lagaron, J. M. *Macromol. Symp.* **2002**, *184*, 19.
40. Rabiej, S.; Binias, W.; Binias, D. *Fibres Text East Eur.* **2008**, *16*, 57.
41. Migler, K. B.; Kotula, A. P.; Hight Walker, A. R. *Macromolecules* **2015**, *48*, 4555.
42. Seguela, R. *J. Polym. Sci. Polym. Phys.* **2005**, *43*, 1729.
43. Chen, T.; Yang, H.; Li, W. *J. Polym. Res.* **2015**, *22*, 1.
44. Soares, J. B. P.; Abbott, R. F.; Kim, J. D. *J. Polym. Sci. Polym. Phys.* **2000**, *38*, 1267.
45. Gautam, S.; Balijepalli, S.; Rutledge, G. C. *Macromolecules* **2000**, *33*, 9136.
46. Balijepalli, S.; Rutledge, G. C. *Comput. Theoret. Polym. Sci.* **2000**, *10*, 103.
47. Migler, K.; Kotula, A.; Hight Walker, A. *APS March Meeting Abstracts*, March 14–18, 2016; Baltimore, Maryland, **2016**.
48. Kim, J. M.; Locker, R.; Rutledge, G. C. *Macromolecules* **2014**, *47*, 2515.
49. Flory, P. J.; Yoon, D. Y. *Nature* **1978**, *272*, 226.
50. Collins, R. A.; Russell, A. F.; Mountford, P. *Appl. Petrochem. Res.* **2015**, *5*, 153.
51. Mueller, P. A.; Richards, J. R.; Congalidis, J. P. *Macromol. React. Eng.* **2011**, *5*, 261.
52. Bubeck, R. A. *Mat. Sci. Eng. R.* **2002**, *39*, 1.
53. Chum, P. S.; Kruper, W. J.; Guest, M. J. *Adv. Mater.* **2000**, *12*, 1759.
54. Suhm, J.; Schneider, M. J.; Mulhaupt, R. J. *Mol. Catal. A: Chem.* **1998**, *128*, 215.
55. Sanchez, K. D.; Allen, N. S.; Liauw, C. M.; Johnson, B. *J. Vinyl Addit. Technol.* **2011**, *17*, 28.
56. Liu, P.; Liu, W.; Wang, W. J.; Li, B. G.; Zhu, S. *Macromol. React. Eng.* **2016**, *10*, 156.
57. Alamo, R. G.; Mandelkern, L. *Thermochim. Acta* **1994**, *238*, 155.
58. Lacher, R. C.; Bryant, J. L. *Macromolecules* **1988**, *21*, 1183.
59. Huang, Y. L.; Brown, N. *J. Polym. Sci. Polym. Phys.* **1991**, *29*, 129.
60. Baker, A. M. E.; Windle, A. H. *Polymer* **2001**, *42*, 667.
61. Rastogi, S.; Terry, A. E. In Interphases and Mesophases in Polymer Crystallization I; Allegra, G., Ed., Springer, Berlin, Germany, **2005**.
62. Balijepalli, S.; Rutledge, G. C. *J. Chem. Phys.* **1998**, *109*, 6523.

63. Sedighiamiri, A.; Van Erp, T. B.; Peters, G. W. M.; Govaert, L. E.; van Dommelen, J. A. W. *J. Polym. Sci. Polym. Phys.* **2010**, *48*, 2173.
64. Tapash, A.; DesLauriers, P. J.; White, J. L. *Macromolecules* **2015**, *48*, 3040.
65. Pawlak, A.; Galeski, A.; Rozanski, A. *Prog. Polym. Sci.* **2014**, *39*, 921.
66. Galeski, A. *Prog. Polym. Sci.* **2003**, *28*, 1643.
67. van Dommelen, J. A. W.; Parks, D. M.; Boyce, M. C.; Brekelmans, W. A. M.; Baaijens, F. P. T. *Polymer* **2003**, *44*, 6089.
68. Rozanski, A.; Galeski, A. *Int. J. Plast.* **2013**, *41*, 14.
69. Deblieck, R. A. C.; van Beek, D. J. M.; Remerie, K.; Ward, I. M. *Polymer* **2011**, *52*, 2979.
70. Michler, G. H.; Balta-Calleja, F. J. Mechanical Properties of Polymers Based on Nanostructure and Morphology; Taylor & Francis: Philadelphia, USA, **2005**.
71. Sedighiamiri, A.; Senden, D. J. A.; Tranchida, D.; Govaert, L. E.; van Dommelen, J. A. W. *Comp. Mater. Sci.* **2014**, *82*, 415.
72. Peterlin, A. *Abstr. Pap. Am. Chem. Soc.* **1979**, *8*, 79.
73. Schneider, K.; Trabelsi, S.; Zafeiropoulos, N. E.; Davies, R.; Riekel, C.; Stamm, M. *Macromol. Symp.* **2006**, *236*, 241.
74. Schrauwen, B. A. G.; Janssen, R. P. M.; Govaert, L. E.; Meijer, H. E. H. *Macromolecules* **2004**, *37*, 6069.
75. Nitta, K.; Takayanagi, M. *Polym. J.* **2006**, *38*, 757.
76. Kuriyagawa, M.; Nitta, K. H. *Polymer* **2011**, *52*, 3469.
77. Mizushima, M.; Kawamura, T.; Takahashi, K.; Nitta, K. *Polym. Test.* **2014**, *38*, 81.
78. Gaucher-Miri, V.; Seguela, R. *Macromolecules* **1997**, *30*, 1158.
79. Brooks, N. W. J.; Mukhtar, M. *Polymer* **2000**, *41*, 1475.
80. Kazmierczak, T.; Galeski, A.; Argon, A. S. *Polymer* **2005**, *46*, 8926.
81. Martin, S.; Exposito, M. T.; Vega, J. F.; Martinez-Salazar, J. *J. Appl. Polym. Sci.* **2013**, *128*, 1871.
82. Bartczak, Z.; Kozanecki, A. *Polymer* **2005**, *46*, 8210.
83. In't Veld, P. J.; Hutter, M.; Rutledge, G. C. *Macromolecules* **2006**, *39*, 439.
84. Newell, J. Essentials of Modern Materials Science and Engineering; Wiley: Hoboken, USA, **2009**.
85. Ferhat-Hamida, Z.; Phuong-Nguyen, H.; Bernazzani, P.; Haine, A.; Delmas, G. *J. Mater. Sci.* **2007**, *42*, 3138.
86. Lagaron, J. M.; Pastor, J. M.; Kip, B. J. *Polymer* **1999**, *40*, 1629.
87. Fu, L. L.; Jiang, Z. Y.; Enderle, H. F.; Lilge, D.; Li, X. H.; Funari, S. S.; Men, Y. F. *J. Polym. Sci. Polym. Phys.* **2014**, *52*, 368.
88. Coates, P. D.; Caton-Rose, P.; Ward, I. M.; Thompson, G. *Sci. China Chem.* **2013**, *56*, 1017.
89. Xiong, B.; Lame, O.; Chenal, J. M.; Rochas, C.; Seguela, R. *Exp. Polym. Lett.* **2016**, *10*, 311.
90. Xiong, B. J.; Lame, O.; Chenal, J. M.; Rochas, C.; Seguela, R.; Vigier, G. *Macromolecules* **2015**, *48*, 2149.
91. Ward, I. M.; Hadley, D. W. An Introduction to the Mechanical Properties of Solid Polymers; John Wiley and Sons: New York, **1993**.
92. Ginzburg, B. M.; Shepelevskii, A. A.; Sultanov, N.; Tuichiev, S. *J. Macromol. Sci. Part B* **2002**, *41*, 357.
93. van Krevelen, D. W.; te Nijenhuis, K. Properties of Polymers; Elsevier: Oxford, UK, **2009**.
94. Ginzburg, B. *J. Macromol. Sci. Part B: Phys.* **2005**, *44*, 217.
95. Lagaron, J. M. *J. Mater. Sci.* **2002**, *37*, 4101.
96. Nitta, K. H.; Nomura, H. *Polymer* **2014**, *55*, 6614.
97. Glenz, W.; Peterlin, A. *J. Polym. Sci. Part A-2: Polym. Phys.* **1971**, *9*, 1243.
98. Naylor, C. C.; Meier, R. J.; Kip, B. J.; Williams, K. P. J.; Mason, S. M.; Conroy, N.; Gerrard, D. L. *Macromolecules* **1995**, *28*, 2969.
99. Lagaron, J. M.; Lopez-Quintana, S.; Rodriguez-Cabello, J. C.; Merino, J. C.; Pastor, J. M. *Polymer* **2000**, *41*, 2999.
100. Afeworki, M.; Brant, P.; Lustiger, A.; Norman, A. *Solid State Nucl. Magn. Reson.* **2015**, *72*, 27.
101. Glenz, W.; Morosoff, N.; Peterlin, A. *J. Polym. Sci. Part B: Polym. Lett.* **1971**, *9*, 211.
102. Sandkuehler, P. The Grass Yarn & Tufters Forum 2008, Zurich, AMI, Bristol-UK, Switzerland, **2008**.
103. Liu, Y. T.; Yin, L. X.; Zhao, H. R.; Song, G. K.; Tang, F. M.; Wang, L. L.; Shao, H. L.; Zhang, Y. P. *J. Appl. Polym. Sci.* **2015**, *132*, 11.
104. Liu, J. M. K.; Nozue, Y.; Nagamatsu, T.; Hosoda, S. *J. Appl. Polym. Sci.* **2007**, *105*, 3673.
105. Patel, R. M. *J. Appl. Polym. Sci.* **2012**, *124*, 1542.
106. Emge, T.; Morton-Finger, J. Google Pat. (**2015**).
107. Villacañas, V.; Sánchez-Sánchez, J.; García-Unanue, J.; López, J.; Gallardo, L. *Proc. Inst. Mech. Eng. Part P: J. Sports Eng. Technol.* **2016**, article in press.
108. George, M.; Reddick, R. S. Google Pat. (**2015**).
109. Rodrigues, L.; Rosendo, H.; Silva, S.; Duraes, N.; Moura, B.; Silva, R.; Moreira, A. In Technical Textiles Magazine. Adrian, W., Ed.; International Newsletters LTD: Doritwich - UK, **2016**, p 22.
110. Wang, X.; Fleming, P. R.; Forrester, S. *Proc. Eng.* **2014**, *72*, 865.
111. Mehravar, M.; Fleming, P.; Cole, D.; Forrester, S. E. The 24th UK Conference of the Association for Computational Mechanics in Engineering, Cardiff University, Cardiff, **2016**.
112. McLaren, N.; Fleming, P.; Forrester, S. *Proc. Eng.* **2012**, *34*, 831.
113. Fleming, P.; Forrester, S. *Proc. Eng.* **2014**, *72*, 925.
114. Forrester, S. E.; Tsui, F. *Proc. Inst. Mech. Eng. Part P: J. Sports Eng. Technol.* **2014**, *228*, 213.
115. Mashburn, L.; Miller, D. R.; Harrison, W. H. Google Pat. (**2015**).